Biochemical and Biophysical Research Communications 441 (2013) 886–890

Contents lists available at ScienceDirect

Biochemical and Biophysical Research Communications

journal homepage: www.elsevier.com/locate/ybbrc

Sclerostin deficient mice rapidly heal bone defects by activating β-catenin and increasing intramembranous ossification

Meghan E. McGee-Lawrence [a], Zachary C. Ryan [b], Lomeli R. Carpio [c], Sanjeev Kakar [a], Jennifer J. Westendorf [a,c], Rajiv Kumar [b,c,*]

[a] Department of Orthopedic Surgery, Mayo Clinic College of Medicine, Mayo Clinic, 200 1st St., Southwest, Rochester, MN 55905, USA
[b] Nephrology Research, Department of Medicine, Mayo Clinic College of Medicine, Mayo Clinic, 200 1st St., Southwest, Rochester, MN 55905, USA
[c] Department of Biochemistry and Molecular Biology, Mayo Clinic College of Medicine, Mayo Clinic, 200 1st St., Southwest, Rochester, MN 55905, USA

ARTICLE INFO

Article history:
Received 23 October 2013
Available online 6 November 2013

Keywords:
Sclerostin
β-Catenin
Wnt
Fracture healing
Osteoblast
Intramembranous ossification

ABSTRACT

We investigated the influence of the osteocyte protein, sclerostin, on fracture healing by examining the dynamics and mechanisms of repair of single-cortex, stabilized femoral defects in sclerostin knockout (*Sost*$^{-/-}$; KO) and sclerostin wild-type (*Sost*$^{+/+}$; WT) mice. Fourteen days following generation of bone defects, *Sost* KO mice had significantly more bone in the healing defect than WT mice. The increase in regenerating bone was due to an increase in the thickness of trabecularized spicules, osteoblast numbers and surfaces within the defect. Enhanced healing of bone defects in *Sost* KO mice was associated with significantly more activated β-catenin expression than observed in WT mice. The findings were similar to those observed in *Axin2*$^{-/-}$ mice, in which β-catenin signaling is known to be enhanced to facilitate bone regeneration. Taken together, these data indicate that enhanced β-catenin signaling is present in *Sost*$^{-/-}$ mice that demonstrate accelerated healing of bone defects, suggesting that modulation of β-catenin signaling in bone could be used to promote fracture repair.

1. Introduction

Fractures are among the most common injuries in people of all ages. The lifetime risk of sustaining a traumatic fracture that must be referred for orthopedic treatment exceeds that of stroke, type 2 diabetes, and either breast or prostate cancer [1]. Fractures reduce mobility, productivity and quality of life. Therefore, interventions that accelerate fracture repair will be of great therapeutic value.

The innate healing capacity of bone tissue is widely recognized. Wnts are potent morphogens and mitogens essential for normal bone formation and fracture healing [2,3]. The canonical Wnt pathway is well recognized as a crucial pathway for proper skeletal development, maintenance of bone mass, and bone regeneration. This pathway dictates osteoblast specification from osteo/chondro-progenitors, inhibits early stages of chondrogenesis, stimulates osteoblast proliferation, enhances osteoblast and osteocyte survival, and transmits mechanical loading signals to bone lining cells [2,4–7]. A simplified description of "canonical" Wnt signaling begins with Wnt ligands binding to receptor complexes consisting of Lrp5/6 and Frizzled (Fzd) proteins [8]. This inactivates a destruction complex composed of Axin1/2, Gsk3β, Disheveled (Dsh), APC and other proteins, leading to β-catenin stabilization and its translocation to the nucleus where it displaces co-repressors from Tcf7 and Lef1 transcription factors and regulates the expression of genes involved in cell proliferation (*e.g.,* cyclin D1) [9], negative feedback (*e.g.,* Axin2) [10], osteoblast differentiation (*e.g.,* osteocalcin) [11] and other activities (*e.g.,* Wisp1, Wisp2). Several secreted proteins (*e.g.,* sclerostin, Dkk1, and Sfrps) prevent Lrp5/6- and/or Wnt-mediated signaling.

Sclerostin is encoded by the *SOST* gene, which is mutated in several genetic disorders of high bone mass and expressed at high levels by osteocytes [12,13]. The seminal discoveries that mutations in *SOST* and *LRP5* alter bone density in humans sparked immense interest in these and other Wnt pathway components [12,14–16]. Canonical Wnt signaling positively regulates proliferation of mesenchymal stem cells that act as the progenitor cell population for the osteoblast lineage [22]. Several studies indicate that sclerostin plays important roles in fracture healing. Sclerostin levels are increased near healing human fracture callus [17]. Genetic deletion of *Sost* [18] or administration of sclerostin-neutralizing antibodies [19] to WT mice accelerated the healing of transverse fractures through endochondral ossification. Anti-sclerostin antibodies also improved bone regeneration in cases of biologically impaired fracture healing, such as type 2 diabetes [20]. Previous studies emphasized the role of sclerostin as an inhibitor of osteogenic canonical Wnt signaling, and as such it might be inferred that β-catenin is

* Corresponding author at: Medical Sciences 1-120, Mayo Clinic, 200 1st St., Southwest, Rochester, MN 55905, USA. Fax: +1 507 538 3954.
E-mail address: rkumar@mayo.edu (R. Kumar).

0006-291X/$ - see front matter © 2013 Elsevier Inc. All rights reserved.
http://dx.doi.org/10.1016/j.bbrc.2013.10.155

required for the anabolic effect of sclerostin inhibition on bone formation. However, the involvement of this intracellular signaling mediator has not been tested or proven *in vivo*.

We recently described a new *Sost*-KO mouse line that has high bone mass due to increased bone mineral accretion and elevated osteoblast numbers [21]. In the current study, we examined the rate and mechanism of defect repair in a fracture model that heals by intramembranous ossification and differentiation of mesenchymal progenitors directly into osteoblast lineage cells. Our studies reveal that *Sost*-KO mice rapidly heal bone defects by activating β-catenin and increasing osteoblast numbers.

2. Materials and methods

All animal research was conducted according to guidelines provided by the National Institutes of Health and the Institute of Laboratory Animal Resources, National Research Council. The Mayo Clinic Institutional Animal Care and Use Committee approved all animal studies. Male WT ($Sost^{+/+}$) and sclerostin-deficient ($Sost^{-/-}$) mice [21] were 13 weeks-old when bone defects were introduced. Male mice deficient in Axin2 ($Axin2^{-/-}$), an intracellular negative feedback inhibitor of canonical Wnt/beta-catenin signaling [23,24] and WT control littermates ($Axin2^{+/+}$) were 8–12 weeks-old at the time of surgery.

2.1. Surgical procedures

Single-cortex, fully stabilized defects were made in the mid-diaphysis of femurs with slight modifications to a previously described protocol [25]. Briefly, mice were anesthetized with isoflurane and prepared for aseptic surgery. Acetaminophen (1 mg/mL) was administered in the drinking water starting 24 h before surgery and thereafter through all experiments. Buprenorphine was provided perioperatively at 0.09 mg/kg via subcutaneous injection. A small incision was made above the mid-diaphysis of the femur, after which the bone was exposed with blunt dissection. A 0.7 mm diameter steel burr drill bit (Fine Science Tools # 19007-07) and an electric drill was used to induce a single-cortex defect in the mid-diaphysis of the femur. Perforations disrupted cortical, periosteal, and endocortical surfaces and extended into the marrow but did not disrupt the opposite cortical wall. Defect healing was monitored via radiography (Faxitron LX-60) on days 7 and 14 after surgery. $Sost^{-/-}$ mice and WT littermates were sacrificed by carbon dioxide inhalation at postoperative day 7 (for immunohistochemistry) or at postoperative day 14 (for histology and quantification of bone architecture). $Axin2^{-/-}$ mice and WT littermates were sacrificed on postoperative day 21.

2.2. Static histomorphometry and microCT

At 14 days ($Sost^{-/-}$ mice and $Sost^{+/+}$ littermates) or 21 days ($Axin2^{-/-}$ mice and $Axin2^{+/+}$ littermates) post-surgery, the mid-diaphysis of each femur (1.6 mm/233 slices), centered about the defect, was scanned in 70% ethanol with a μCT35 scanner (Scanco Medical AG, Basserdorf, Switzerland) at 7 μm voxel size using an energy setting of 70 kVp and an integration time of 300 ms [26–28]. Longitudinal views from the center of the defect were generated an analyzed with image analysis software (Bioquant Osteo,

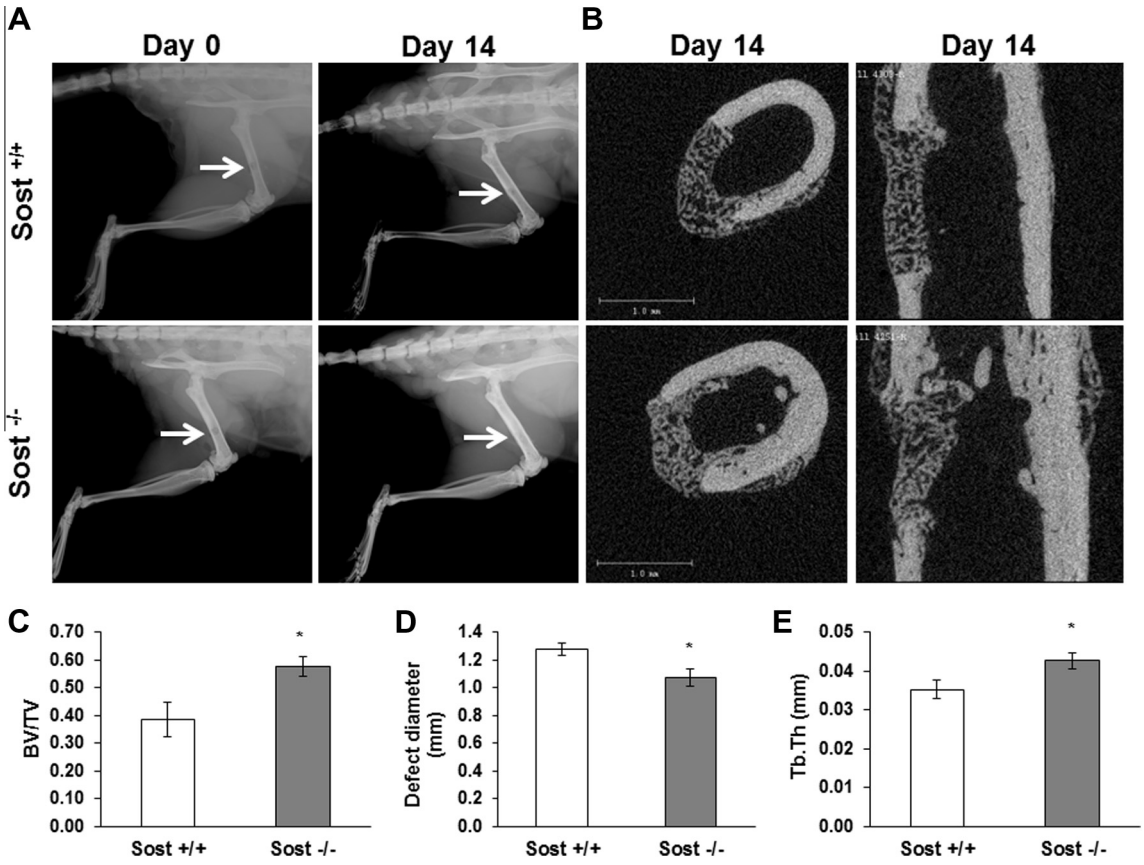

Fig. 1. Bone defect healing is accelerated in $Sost^{-/-}$ mice. (A) X-rays were taken of femurs immediately (day 0) and 14 days after surgical induction of single-cortex defects. The arrow indicates the site of the bone defect. (B) MicroCT reconstructions of the defect at postoperative day 14. (C) Bone volume fraction within the defect was calculated from the microCT reconstructions at day 14. (D) Defect diameter was calculated with image analysis software from longitudinal views of the microCT reconstructions at day 14. (E) The thickness of regenerated spicules (trabeculae) in the bone defect was calculated from the microCT reconstructions at day 14. $^{*}p < 0.05$.

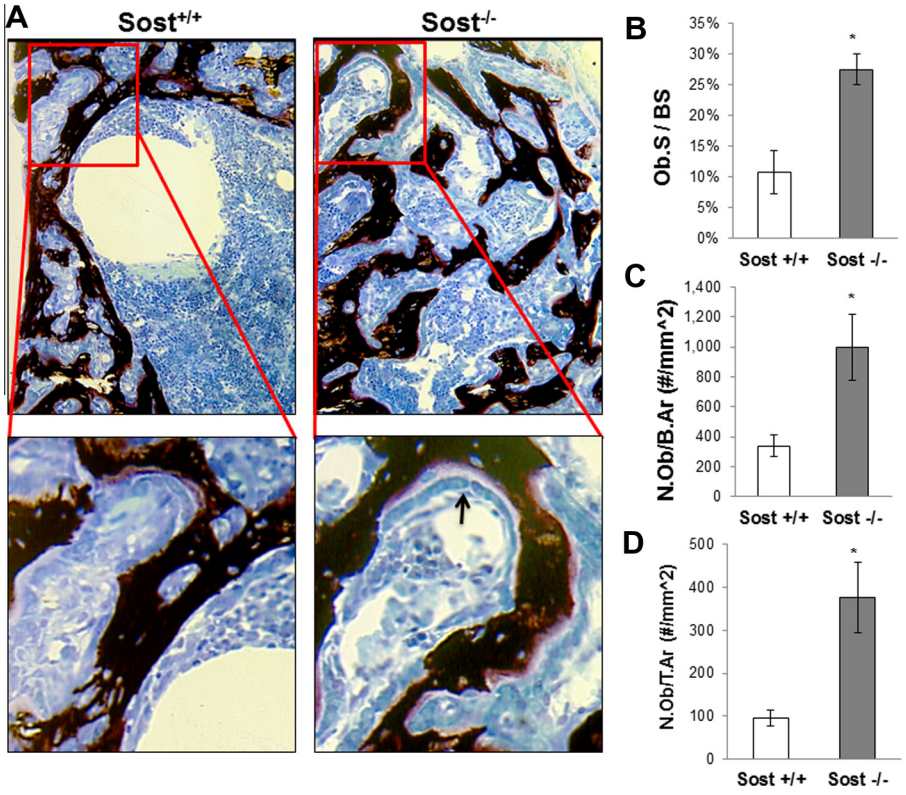

Fig. 2. Osteoblast numbers are elevated in defects of Sost$^{-/-}$ mice. (A) Bone histological sections through the defect (postoperative day 14) were stained with Von Kossa/MacNeal's tetrachrome. The arrow points to active osteoblasts producing osteoid. (B–D) Osteoblast surface area per bone surface area (Ob.S/BS), the number of osteoblasts per bone area (N.Ob/B.Ar), and number of osteoblasts per tissue area (N.Ob/T.Ar) within the defect were measured by histomorphometry. $^{*}p < 0.05$.

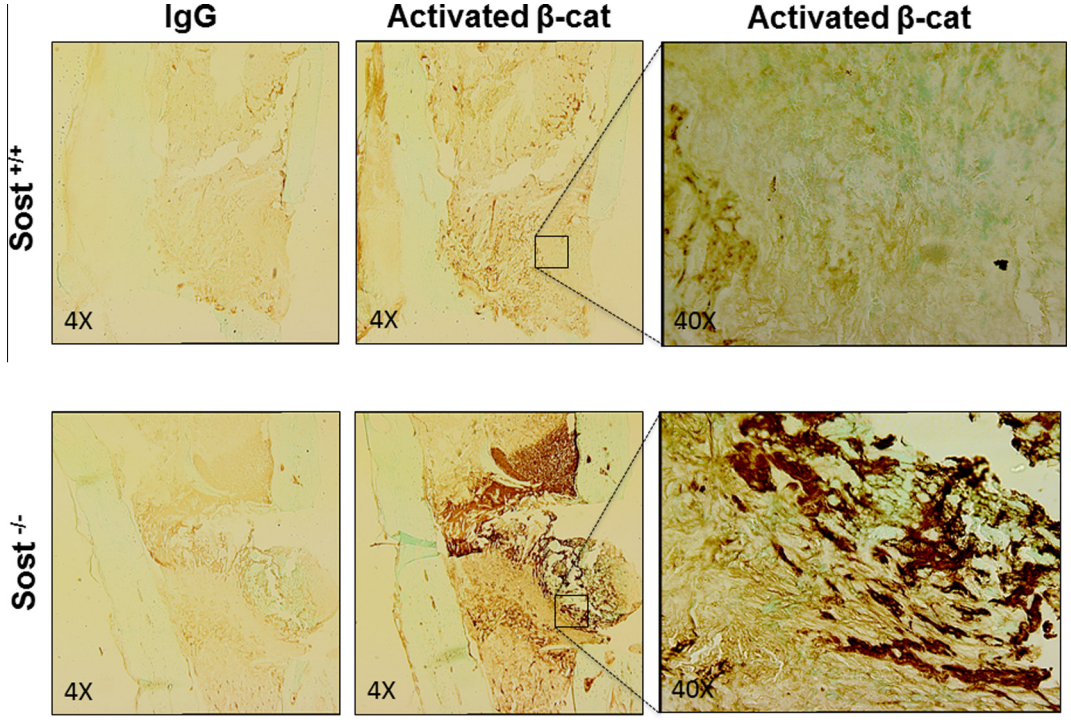

Fig. 3. β-Catenin levels are elevated in defects of Sost$^{-/-}$ mice. Immunohistochemistry was performed on specimens from postoperative day 7 with an antibody that recognizes β-catenin molecules that are un-phosphorylated at Ser33/37 and Thr41 or an isotype control antibody (Rabbit IgG).

Nashville, TN) to quantify defect diameter. The central region (30 slices, 0.21 mm long) of each scan from the *Sost*$^{-/-}$ mice and *Sost*$^{+/+}$ littermates was selected for analysis of bone microarchitecture. Trabecular bone volume fraction (Tb.BV/TV, %), trabecular number (Tb.N, mm^{-1}), trabecular thickness (Tb.Th, mm), and trabecular separation (Tb.Sp, mm), were computed using the manufacturer's software (Sigma = 0.8, Support = 1, Threshold = 220). Samples were subsequently histologically prepared. Thin (5 μm) undecalcified longitudinal bone sections were prepared through the center of the dealing defect. Sections from the *Sost*$^{-/-}$ mice and *Sost*$^{+/+}$ littermates were stained with VonKossa/MacNeal's tetrachrome to highlight osteoblast surfaces [29]. Osteoblastic histomorphometric indices were measured across the entire defect. Slides were digitized using a microscope and digital camera and analyzed using image analysis software at 200× magnification (Bioquant Osteo). Osteoblast surface/bone surface (Ob.S/BS, %), osteoblast number per bone area (N.Ob/B.Ar #/mm^2) and osteoblast number per tissue area (N.Ob/T.Ar #/mm^2) were quantified from the stained sections. Histological sections from *Axin2*$^{-/-}$ mice and *Axin2*$^{+/+}$ littermates were stained with Safranin O/Light Green for qualitative analysis at postoperative day 21.

2.3. Immunohistochemistry

Femurs were fixed in 10% neutral buffered formalin and decalcified for 7 days in 15% EDTA; complete decalcification was confirmed by X-ray. Decalcified bones were embedded in paraffin and sectioned longitudinally through the defect at a thickness of 8 microns. Immunohistochemical staining was performed with monoclonal antibodies directed to activated form of beta-catenin that is un-phosphorylated on Ser33/37 and Thr41 (D13A1, Cell Signaling #8814, 1:50 dilution), or an IgG isotype control (Vector Laboratories I-1000). Chromogens were developed using a polyvalent secondary HRP detection kit (Abcam, ab93697) followed by 3′-3′-diaminobenzidine (DAB) (Sigma–Aldrich), and then counterstained with fast green.

2.4. Statistics

Statistics were performed with JMP 9.0 statistical analysis software (SAS Institute Inc., Cary, NC). Data were compared between groups within each experiment with Student's *t*-tests using a significance of $p < 0.05$ for all comparisons.

3. Results and discussion

As previously reported, *Sost*$^{-/-}$ animals presented with noticeably enhanced bone mass as compared to WT (*Sost*$^{+/+}$) controls at 13 weeks of age (Fig. 1; note differences in cortical bone thickness between *Sost*$^{+/+}$ and *Sost*$^{-/-}$ animals) [21]. Surgical defects were successfully induced in mice from both groups (Fig. 1A). Fourteen days after surgery, *Sost*$^{-/-}$ animals had significantly more bone in the healing defect as compared to *Sost*$^{+/+}$ controls (Fig. 1A and B). MicroCT analysis confirmed an increase in bone volume fraction at the defect site (+49%, $p = 0.021$; Fig. 1C) and a reduction in the defect diameter (Fig. 1D). This increase in regenerated bone was largely due to an increase in the thickness of trabecularized spicules, as Tb.Th within the defect was significantly (+21%) greater in *Sost*$^{-/-}$ as compared to wild-type *Sost*$^{+/+}$ mice (Fig. 1E). In contrast, no differences were seen in the number (+8%, $p = 0.342$) or spacing (−19%, $p = 0.242$) of bone struts between *Sost*$^{-/-}$ and *Sost*$^{+/+}$ mice. These data are consistent with the previously reported developmental phenotype, which showed significantly thicker trabeculae (+49%) in the metaphysis of the distal femur as compared to WT littermates at 8 weeks of age, with no differences in trabecular number or separation [21].

Histomorphometric analyses revealed a significant increase in osteoblast surface (+155% $p = 0.004$) and osteoblast numbers, whether normalized to bone area (+193%, $p = 0.045$) or tissue area (+291%, $p = 0.027$) within the defect site in the *Sost*$^{-/-}$ mice as compared to *Sost*$^{+/+}$ littermates (Fig. 2). These results indicate that the rapid healing in the *Sost*$^{-/-}$ animals may be attributed to a greater population of osteoblast-lineage cells available to generate new bone.

To gain insight into mechanisms of rapid healing in the *Sost*$^{-/-}$ animals, immunohistochemistry was performed at postoperative day 7 to detect the presence of activated β-catenin, the non-phosphorylated form of β-catenin that is capable of translocating to the nucleus and increasing expression of Wnt-responsive target genes. Active β-catenin staining was more intense within the defect of *Sost*$^{-/-}$ mice than in *Sost*$^{+/+}$ animals (Fig. 3).

Finally, we compared the healing response of *Sost*$^{-/-}$ mice to another animal model with enhanced β-catenin signaling. *Axin2*$^{-/-}$ mice demonstrate high osteoblastic bone formation activity in both axial and appendicular skeletal sites due to enhanced canonical Wnt/β-catenin signaling that increases progenitor cell proliferation [22,24,30]. We previously reported that bone marrow-derived osteoblast progenitors from *Axin2*$^{-/-}$ animals rapidly

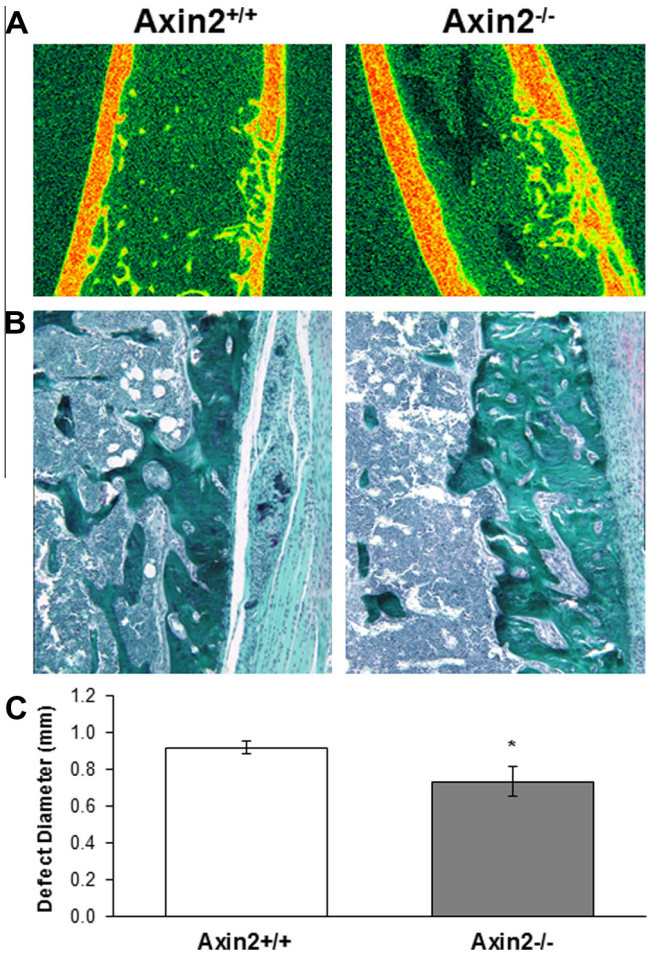

Fig. 4. Bone defect healing is accelerated in *Axin2*$^{-/-}$ mice. (A) MicroCT reconstructions of defects in wild-type (*Axin2*$^{+/+}$) and *Axin2*$^{-/-}$ mice at postoperative day 21. (B) Histological sections of defects in wild-type (*Axin2*$^{+/+}$) and *Axin2*$^{-/-}$ mice at postoperative day 21 stained with Safranin O/Light Green. (C) Quantitative assessment of defect diameter. Defect diameter was calculated with image analysis software from longitudinal views of the microCT reconstructions.

differentiate into matrix producing osteoblasts with enhanced production of key osteoblast genes like *Runx2* and *Osteocalcin* [24]. Similar to the *Sost*$^{-/-}$ mice, *Axin2*$^{-/-}$ animals demonstrated rapid healing of the surgical defect via intramembranous bone repair, resulting in a significantly smaller defect diameter as compared to *Axin2*$^{+/+}$ littermates at postoperative day 21 (Fig. 4). These data are consistent with a previous, comprehensive investigation of defect repair in the tibia of *Axin2*$^{-/-}$ animals, where *Axin2*$^{-/-}$ mice displayed increased cell proliferation and earlier expression of osteoblastic markers like type I collagen and alkaline phosphatase as compared to WT controls [31].

In summary, *Sost* deficiency enhances intramembranous bone repair by stabilizing β-catenin levels and increasing osteoblast numbers. These data suggest that early and localized administration of anti-sclerostin therapies or other therapeutic agents that up-regulate canonical Wnt/β-catenin signaling could accelerate fracture healing.

Acknowledgments

The NIH (R01 DE020194, AR60869, T32 AR056950, F32 AR60140) a grant from the Dr. Ralph and Marion Falk Foundation and the Mayo Clinic Center for Regenerative Medicine supported this work. The authors thank David Razidlo and Bridget Stensgard for assistance with surgical procedures and mouse colony maintenance, and the Mayo Clinic Biomaterials and Quantitative Histomorphometry Core Laboratory for assistance with histological specimen preparation.

References

[1] M.R. Brinker, D.P. O'Connor, The incidence of fractures and dislocations referred for orthopaedic services in a capitated population, J. Bone Joint Surg. Am. 86-A (2004) 290–297.
[2] D.G. Monroe, M.E. McGee-Lawrence, M.J. Oursler, J.J. Westendorf, Update on Wnt signaling in bone cell biology and bone disease, Gene 492 (2012) 1–18.
[3] F.J. Secreto, L.H. Hoeppner, J.J. Westendorf, Wnt signaling during fracture repair, Curr. Osteoporos. Rep. 7 (2009) 64–69.
[4] S. Khosla, J.J. Westendorf, M.J. Oursler, Building bone to reverse osteoporosis and repair fractures, J. Clin. Invest. 118 (2008) 421–428.
[5] L.F. Bonewald, M.L. Johnson, Osteocytes, mechanosensing and Wnt signaling, Bone 42 (2008) 606–615.
[6] B.O. Williams, K.L. Insogna, Where Wnts went: the exploding field of Lrp5 and Lrp6 signaling in bone, J. Bone Miner. Res. 24 (2009) 171–178.
[7] L.H. Hoeppner, F.J. Secreto, J.J. Westendorf, Wnt signaling as a therapeutic target for bone diseases, Expert Opin. Ther. Targets 13 (2009) 485–496.
[8] J.J. Westendorf, R.A. Kahler, T.M. Schroeder, Wnt signaling in osteoblasts and bone diseases, Gene 341 (2004) 19–39.
[9] M. Shtutman, J. Zhurinsky, I. Simcha, C. Albanese, M. D'Amico, R. Pestell, A. Ben-Ze'ev, The cyclin D1 gene is a target of the beta-catenin/LEF-1 pathway, Proc. Natl. Acad. Sci. USA 96 (1999) 5522–5527.
[10] E.H. Jho, T. Zhang, C. Domon, C.K. Joo, J.N. Freund, F. Costantini, Wnt/beta-catenin/Tcf signaling induces the transcription of Axin2, a negative regulator of the signaling pathway, Mol. Cell. Biol. 22 (2002) 1172–1183.
[11] R.A. Kahler, J.J. Westendorf, Lymphoid enhancer factor-1 and beta-catenin inhibit Runx2-dependent transcriptional activation of the osteocalcin promoter, J. Biol. Chem. 278 (2003) 11937–11944.
[12] W. Balemans, M. Ebeling, N. Patel, E. Van Hul, P. Olson, M. Dioszegi, C. Lacza, W. Wuyts, J. Van Den Ende, P. Willems, A.F. Paes-Alves, S. Hill, M. Bueno, F.J. Ramos, P. Tacconi, F.G. Dikkers, C. Stratakis, K. Lindpaintner, B. Vickery, D. Foernzler, W. Van Hul, Increased bone density in sclerosteosis is due to the deficiency of a novel secreted protein (SOST), Hum. Mol. Genet. 10 (2001) 537–543.
[13] W. Balemans, N. Patel, M. Ebeling, E. Van Hul, W. Wuyts, C. Lacza, M. Dioszegi, F.G. Dikkers, P. Hildering, P.J. Willems, J.B. Verheij, K. Lindpaintner, B. Vickery, D. Foernzler, W. Van Hul, Identification of a 52 kb deletion downstream of the SOST gene in patients with van Buchem disease, J. Med. Genet. 39 (2002) 91–97.
[14] Y. Gong, R.B. Slee, N. Fukai, G. Rawadi, S. Roman-Roman, A.M. Reginato, H. Wang, T. Cundy, F.H. Glorieux, D. Lev, M. Zacharin, K. Oexle, J. Marcelino, W. Suwairi, S. Heeger, G. Sabatakos, S. Apte, W.N. Adkins, J. Allgrove, M. Arslan-Kirchner, J.A. Batch, P. Beighton, G.C. Black, R.G. Boles, L.M. Boon, C. Borrone, H.G. Brunner, G.F. Carle, B. Dallapiccola, A. De Paepe, B. Floege, M.L. Halfhide, B. Hall, R.C. Hennekam, T. Hirose, A. Jans, H. Juppner, C.A. Kim, K. Keppler-Noreuil, A. Kohlschuetter, D. LaCombe, M. Lambert, E. Lemyre, T. Letteboer, L. Peltonen, R.S. Ramesar, M. Romanengo, H. Somer, E. Steichen-Gersdorf, B. Steinmann, B. Sullivan, A. Superti-Furga, W. Swoboda, M.J. van den Boogaard, W. Van Hul, M. Vikkula, M. Votruba, B. Zabel, T. Garcia, R. Baron, B.R. Olsen, M.L. Warman, LDL receptor-related protein 5 (LRP5) affects bone accrual and eye development, Cell 107 (2001) 513–523.
[15] L.M. Boyden, J. Mao, J. Belsky, L. Mitzner, A. Farhi, M.A. Mitnick, D. Wu, K. Insogna, R.P. Lifton, High bone density due to a mutation in LDL-receptor-related protein 5, N. Engl. J. Med. 346 (2002) 1513–1521.
[16] R.D. Little, J.P. Carulli, R.G. Del Mastro, J. Dupuis, M. Osborne, C. Folz, S.P. Manning, P.M. Swain, S.C. Zhao, B. Eustace, M.M. Lappe, L. Spitzer, S. Zweier, K. Braunschweiger, Y. Benchekroun, X. Hu, R. Adair, L. Chee, M.G. FitzGerald, C. Tulig, A. Caruso, N. Tzellas, A. Bawa, B. Franklin, S. McGuire, X. Nogues, G. Gong, K.M. Allen, A. Anisowicz, A.J. Morales, P.T. Lomedico, S.M. Recker, P. Van Eerdewegh, R.R. Recker, M.L. Johnson, A mutation in the LDL receptor-related protein 5 gene results in the autosomal dominant high-bone-mass trait, Am. J. Hum. Genet. 70 (2002) 11–19.
[17] K. Sarahrudi, A. Thomas, C. Albrecht, S. Aharinejad, Strongly enhanced levels of sclerostin during human fracture healing, J. Orthop. Res. 30 (2012) 1549–1555.
[18] C. Li, M.S. Ominsky, H.L. Tan, M. Barrero, Q.T. Niu, F.J. Asuncion, E. Lee, M. Liu, W.S. Simonet, C. Paszty, H.Z. Ke, Increased callus mass and enhanced strength during fracture healing in mice lacking the sclerostin gene, Bone 49 (2011) 1178–1185.
[19] L. Cui, H. Cheng, C. Song, C. Li, W.S. Simonet, H.Z. Ke, G. Li, Time-dependent effects of sclerostin antibody on a mouse fracture healing model, J. Musculoskelet. Neuronal Interact. 13 (2013) 178–184.
[20] C. Hamann, M. Rauner, Y. Hohna, R. Bernhardt, J. Mettelsiefen, C. Goettsch, K.P. Gunther, M. Stolina, C.Y. Han, F.J. Asuncion, M.S. Ominsky, L.C. Hofbauer, Sclerostin antibody treatment improves bone mass, bone strength, and bone defect regeneration in rats with type 2 diabetes mellitus, J. Bone Miner. Res. 28 (2013) 627–638.
[21] Z.C. Ryan, H. Ketha, M.S. McNulty, M. McGee-Lawrence, T.A. Craig, J.P. Grande, J.J. Westendorf, R.J. Singh, R. Kumar, Sclerostin alters serum vitamin D metabolite and fibroblast growth factor 23 concentrations and the urinary excretion of calcium, Proc. Natl. Acad. Sci. USA 110 (2013) 6199–6204.
[22] B. Liu, H.M. Yu, W. Hsu, Craniosynostosis caused by Axin2 deficiency is mediated through distinct functions of beta-catenin in proliferation and differentiation, Dev. Biol. 301 (2007) 298–308.
[23] W. Hsu, R. Shakya, F. Costantini, Impaired mammary gland and lymphoid development caused by inducible expression of Axin in transgenic mice, J. Cell Biol. 155 (2001) 1055–1064.
[24] M.E. McGee-Lawrence, X. Li, K.L. Bledsoe, H. Wu, J.R. Hawse, M. Subramaniam, D.F. Razidlo, B.A. Stensgard, G.S. Stein, A.J. van Wijnen, J.B. Lian, W. Hsu, J.J. Westendorf, Runx2 protein represses Axin2 expression in osteoblasts and is required for craniosynostosis in Axin2-deficient mice, J. Biol. Chem. 288 (2013) 5291–5302.
[25] L. Monfoulet, B. Rabier, O. Chassande, J.C. Fricain, Drilled hole defects in mouse femur as models of intramembranous cortical and cancellous bone regeneration, Calcif. Tissue Int. 86 (2010) 72–81.
[26] S.F. Bensamoun, J.R. Hawse, M. Subramaniam, B. Ilharreborde, A. Bassillais, C.L. Benhamou, D.G. Fraser, M.J. Oursler, P.C. Amadio, K.N. An, T.C. Spelsberg, TGFbeta inducible early gene-1 knockout mice display defects in bone strength and microarchitecture, Bone 39 (2006) 1244–1251.
[27] M.L. Bouxsein, S.K. Boyd, B.A. Christiansen, R.E. Guldberg, K.J. Jepsen, R. Muller, Guidelines for assessment of bone microstructure in rodents using micro-computed tomography, J. Bone Miner. Res. 25 (2010) 1468–1486.
[28] M.L. Bouxsein, T. Uchiyama, C.J. Rosen, K.L. Shultz, L.R. Donahue, C.H. Turner, S. Sen, G.A. Churchill, R. Muller, W.G. Beamer, Mapping quantitative trait loci for vertebral trabecular bone volume fraction and microarchitecture in mice, J. Bone Miner. Res. 19 (2004) 587–599.
[29] M.E. McGee-Lawrence, E.W. Bradley, A. Dudakovic, S.W. Carlson, Z.C. Ryan, R. Kumar, M. Dadsetan, M.J. Yaszemski, Q. Chen, K.N. An, J.J. Westendorf, Histone deacetylase 3 is required for maintenance of bone mass during aging, Bone 52 (2013) 296–307.
[30] Y. Yan, D. Tang, M. Chen, J. Huang, R. Xie, J.H. Jonason, X. Tan, W. Hou, D. Reynolds, W. Hsu, S.E. Harris, J.E. Puzas, H. Awad, R.J. O'Keefe, B.F. Boyce, D. Chen, Axin2 controls bone remodeling through the beta-catenin-BMP signaling pathway in adult mice, J. Cell Sci. 122 (2009) 3566–3578.
[31] S. Minear, P. Leucht, J. Jiang, B. Liu, A. Zeng, C. Fuerer, R. Nusse, J.A. Helms, Wnt proteins promote bone regeneration, Sci. Transl. Med. 2 (2010) (29ra30).